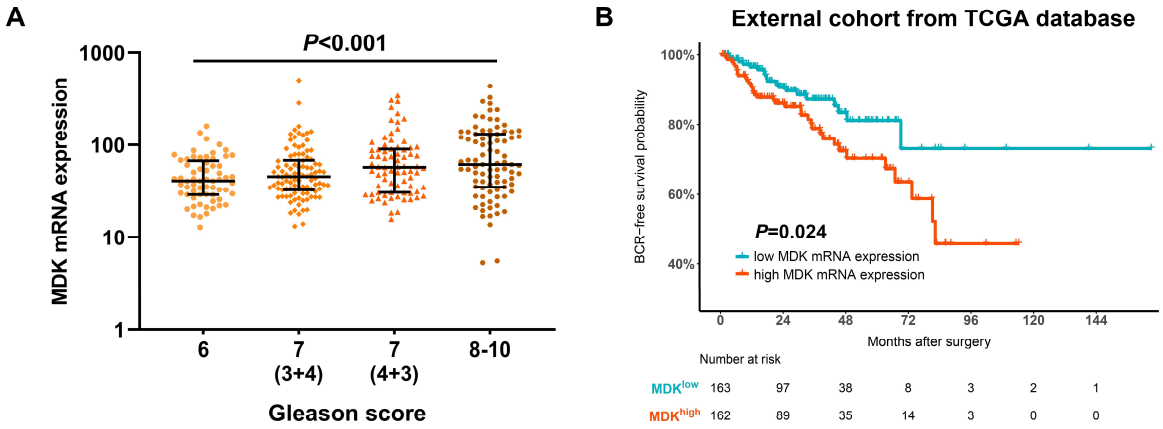

Supplementary Figure 1. MDK expression correlated with Gleason score and an inferior prognosis in external cohort.

(A) Comparison of MDK mRNA expression in Gleason score 6, 7 (3+4), 7 (4+3) and 8-10. (B) The Kaplan-Meier curve for BCR-free survival comparing tumor with high vs. low MDK mRNA expression in external cohort (n=325).

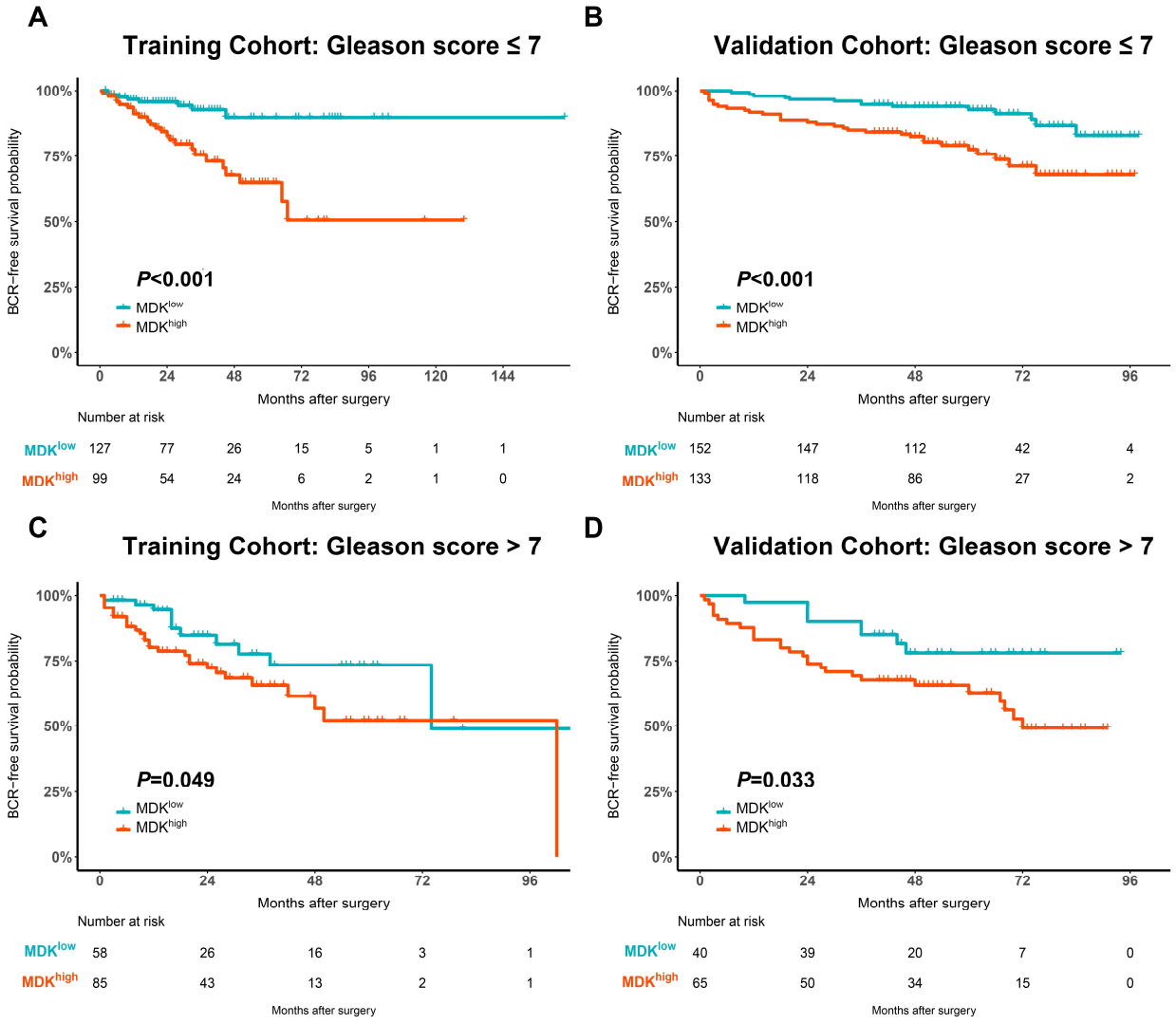

Supplementary Figure 2. Intratumoral MDK expression was associated with poor prognosis in PCa with Gleason score <7 or ≥7 subgroups.

Kaplan-Meier curves for BCR-free survival comparing tumor with high vs. low intratumoral MDK expression in Gleason score <7 subgroups in training cohort (A) and validation cohort (B) or in Gleason score ≥7 subgroups in training cohort (C) and validation cohort (D). Log-rank P values were shown.

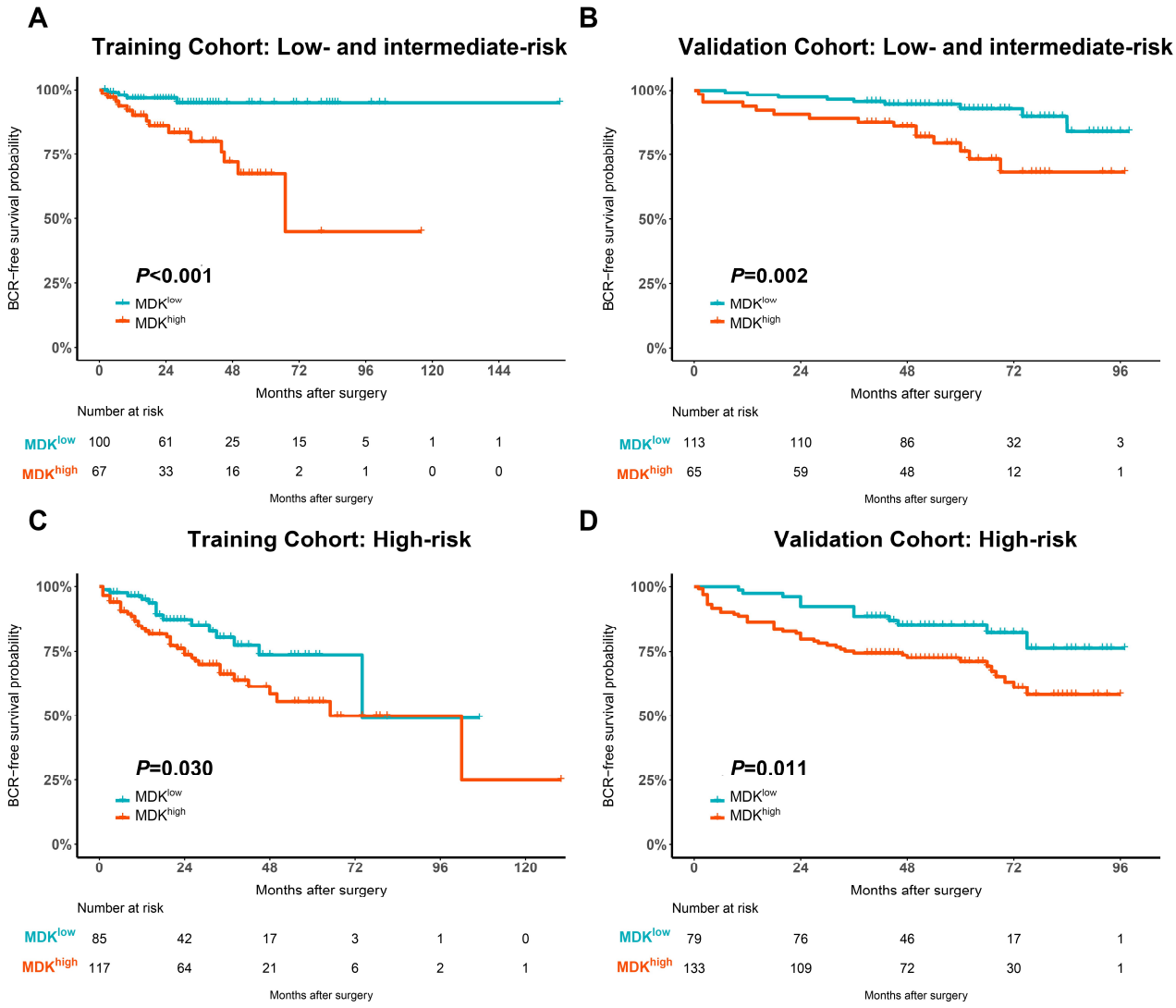

Supplementary Figure 3. Intratumoral MDK expression was associated with poor prognosis in PCa with low- and intermediate-risk or high-risk subgroups.

Kaplan-Meier curves for BCR-free survival comparing tumor with high vs. low intratumoral MDK expression in low- and intermediate-risk subgroups in training cohort (A) and validation cohort (B) or in high-risk subgroups in training cohort (C) and validation cohort (D). Log-rank P values were shown.

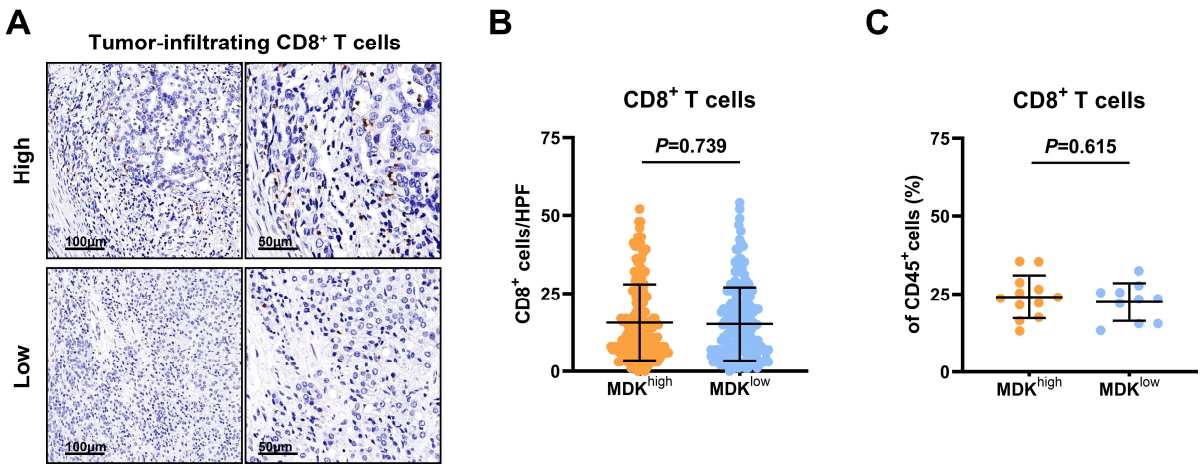

Supplementary Figure 4. $CD8^+$ T cells infiltration in PCa with high/low intratumoral MDK expression.

(A) Representative images showing the high/low infiltration of $CD8^+$ T cells in PCa. (B) Evaluation of $CD8^+$ T cells in tumor with high vs. low MDK expression based on IHC. (C) Evaluation of $CD8^+$ T cells among $CD45^+$ cells in tumor with high vs. low MDK expression through flow cytometry. Data were analyzed with Mann-Whitney U test.

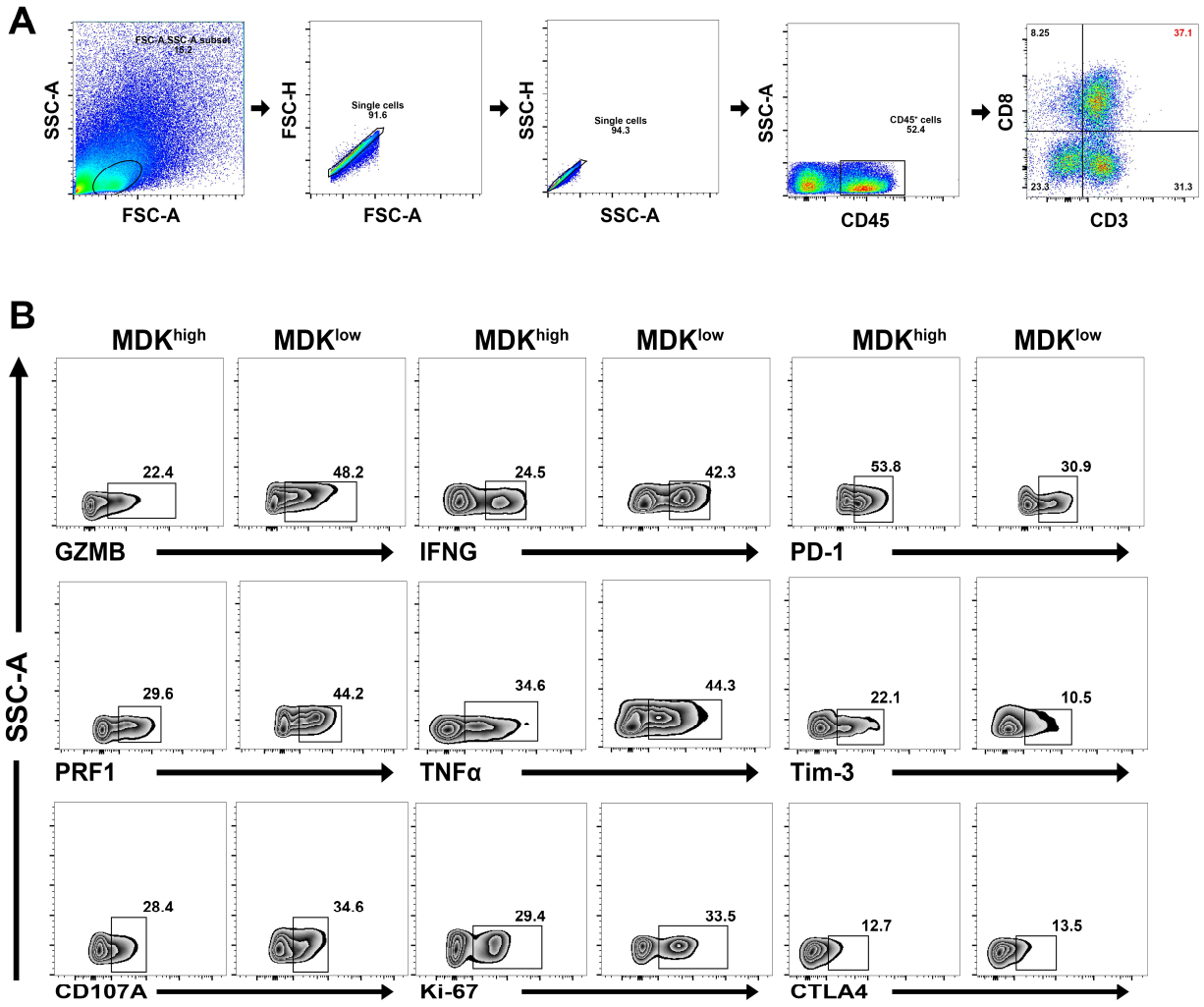

Supplementary Figure 5. Gating strategy and representative flow cytometry images for tumor-infiltrating CD8⁺ T cell in PCa.

(A) Gating strategy for selecting tumor-infiltrating CD8⁺ T cell (CD45⁺ CD3⁺ CD8⁺ cell) in PCa. (B) Representative flow cytometry plots for cytotoxicity, effector, proliferative and immune checkpoint molecules on CD8⁺ T cells in high and low MDK expression groups.

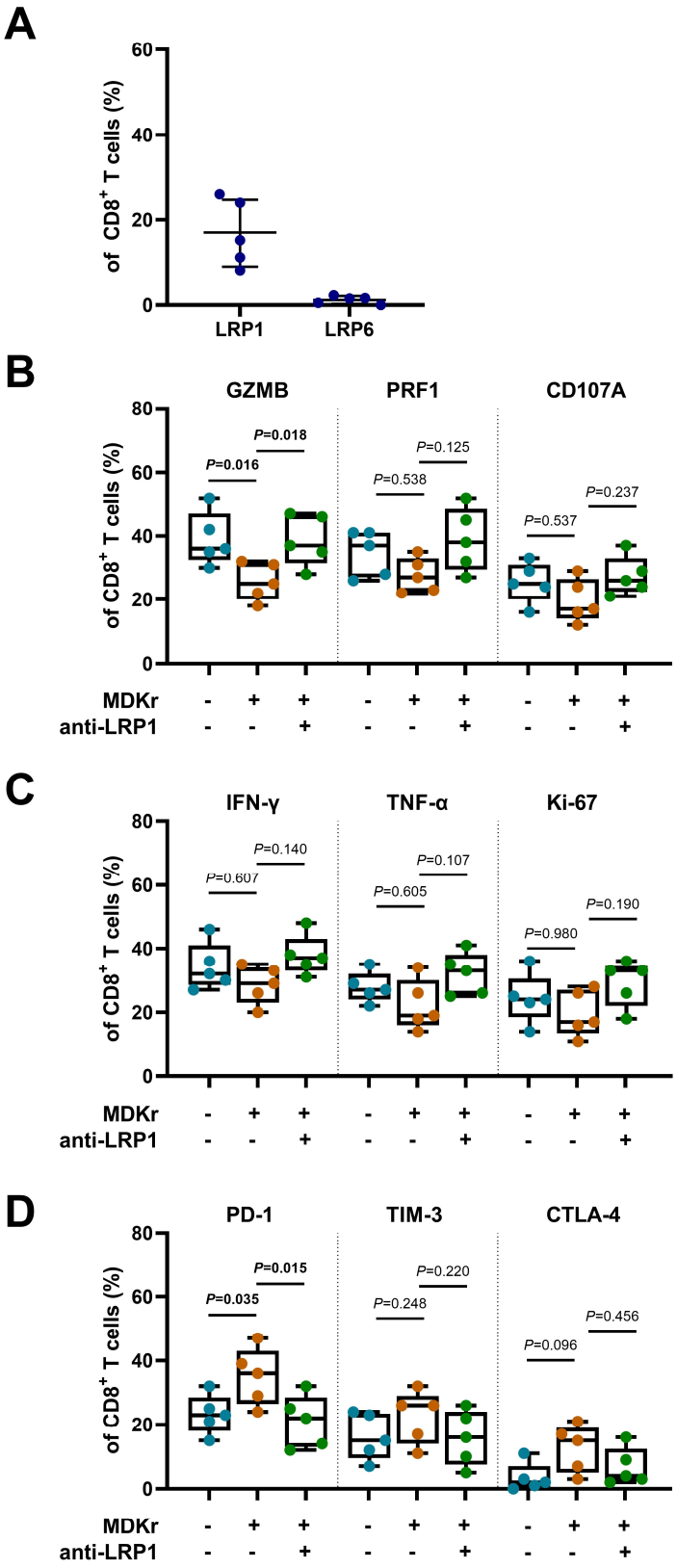

Supplementary Figure 6. MDK showed direct but faint immunosuppressive

effect on CD8$^+$ T cells.

(A) Evaluation of LRP1 and LRP6 expression on CD8$^+$ T cells isolated from PBMCs from patients with tumor (n=5). (B) Evaluation of cytotoxicity expression (GZMB, PRF1 and CD107A) of PBMC-isolated CD8$^+$ T cells treated with MDKr and anti-LRP1. (C) Evaluation of effector expression (IFNG and TNF-α) and proliferative marker (Ki-67) of PBMC-isolated CD8$^+$ T cells treated with MDKr and anti-LRP1. (D) Evaluation of immune checkpoint (PD-1, Tim-3 and CTLA4) of PBMC-isolated CD8$^+$ T cells treated with MDKr and anti-LRP1. Data were analyzed with one-way ANOVA test with Bonferroni correction.

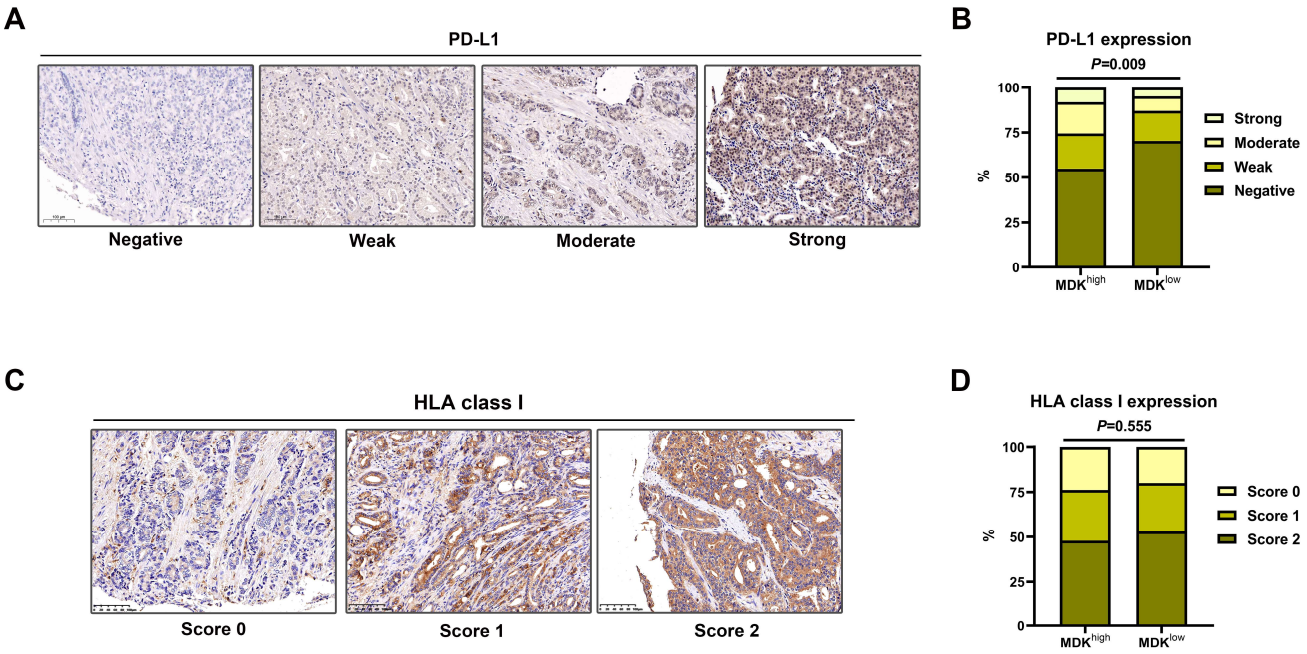

Supplementary Figure 7. High expression of PD-L1 was observed in tumor with high intratumoral MDK expression.

(A) Representative images of PD-L1 through IHC staining. (B) Evaluation of PD-L1 expression in tumor with high/low intratumoral MDK expression. (C) Representative images of HLA Class I through IHC staining. (D) Evaluation of HLA Class I expression in tumor with high/low intratumoral MDK expression. Data was analyzed by Chi-square test.

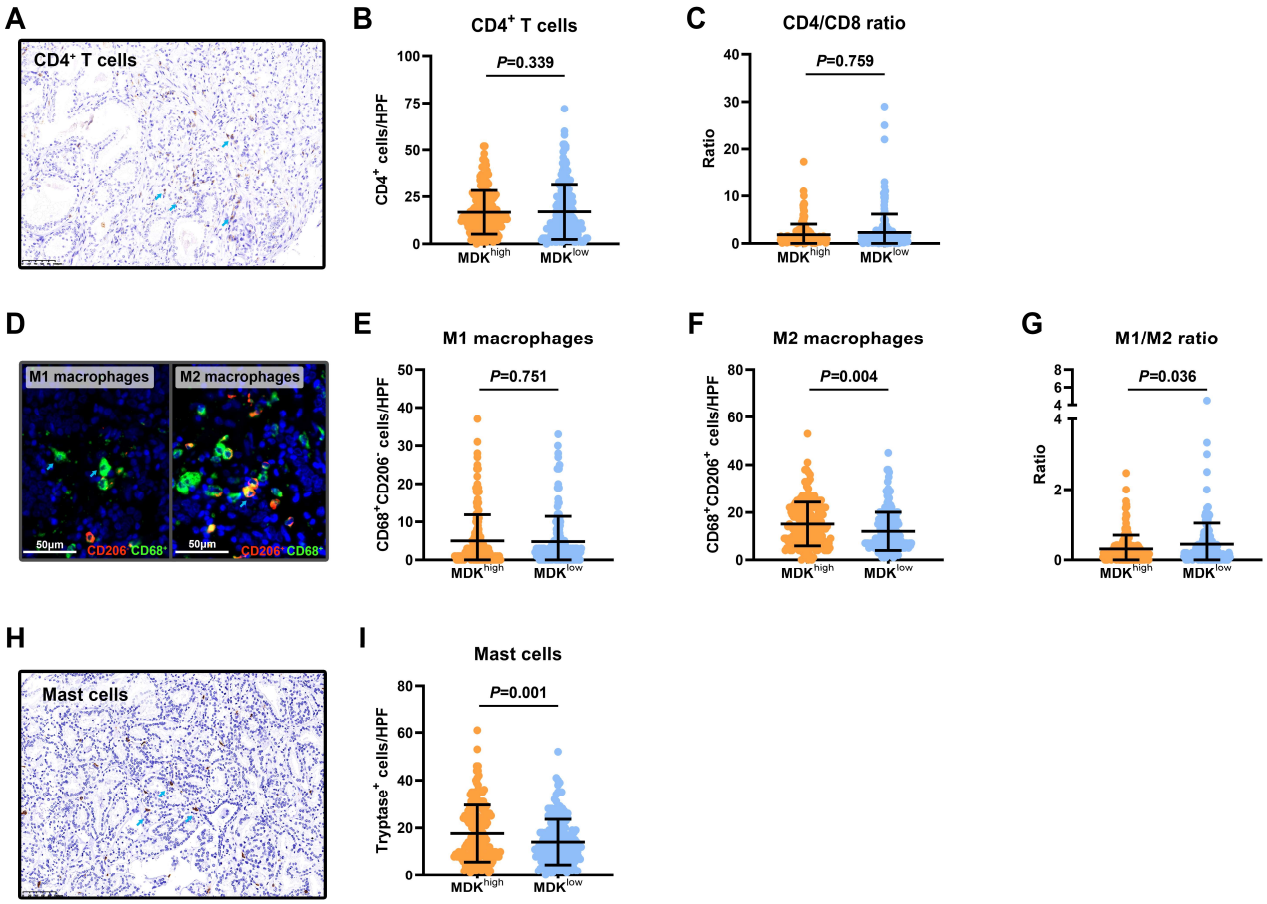

Supplementary Figure 8. Tumor with high MDK expression featured with immunosuppressive immune contexture.

(A) The representative image of $CD4^+$ T cells through IHC staining. (B-C) Evaluation of $CD4^+$ T cell infiltration (B) and CD4/CD8 ratio (C) between tumor with high vs. low MDK expression. (D) The representative image of M1 macrophages ($CD68^+CD206^-$ cells) and M2 macrophages ($CD68^+CD206^+$ cells) through immunofluorescence staining. (E-G) Evaluation of M1 macrophages (E) and M2 macrophages (F) infiltration and M1/M2 ratio (G) between tumor with high vs. low MDK expression. (H) The representative image of mast cells ($Tryptase^+$ cells) through IHC staining. (I) Evaluation of mast cells infiltration between tumor with high vs. low MDK expression. Data was analyzed by Mann-Whitney U test.

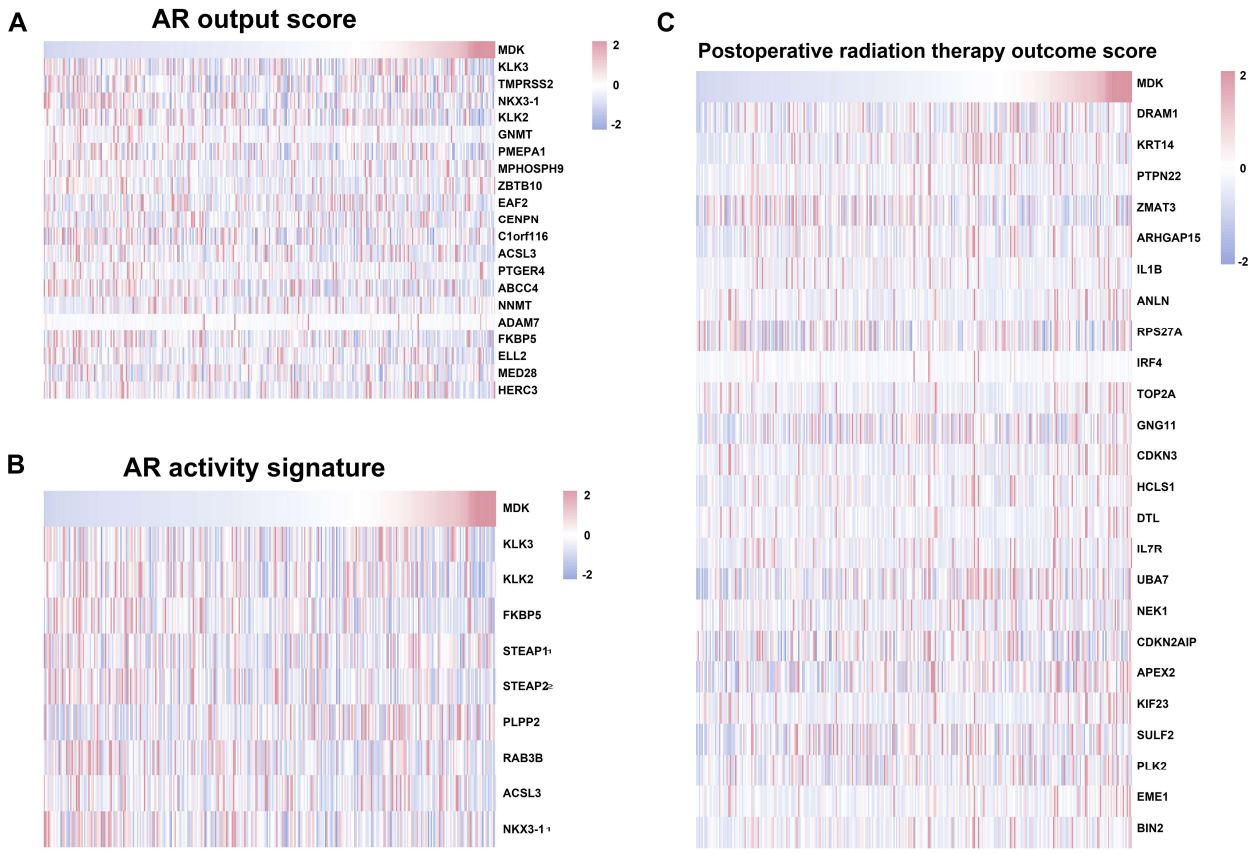

Supplementary Figure 9. Heatmap of signatures associated with therapeutic response.

Heatmap illustrating the MDK expression with AR output score (A), AR activity signature (B), postoperative radiation therapy outcome score (C) in external cohort (n=325).

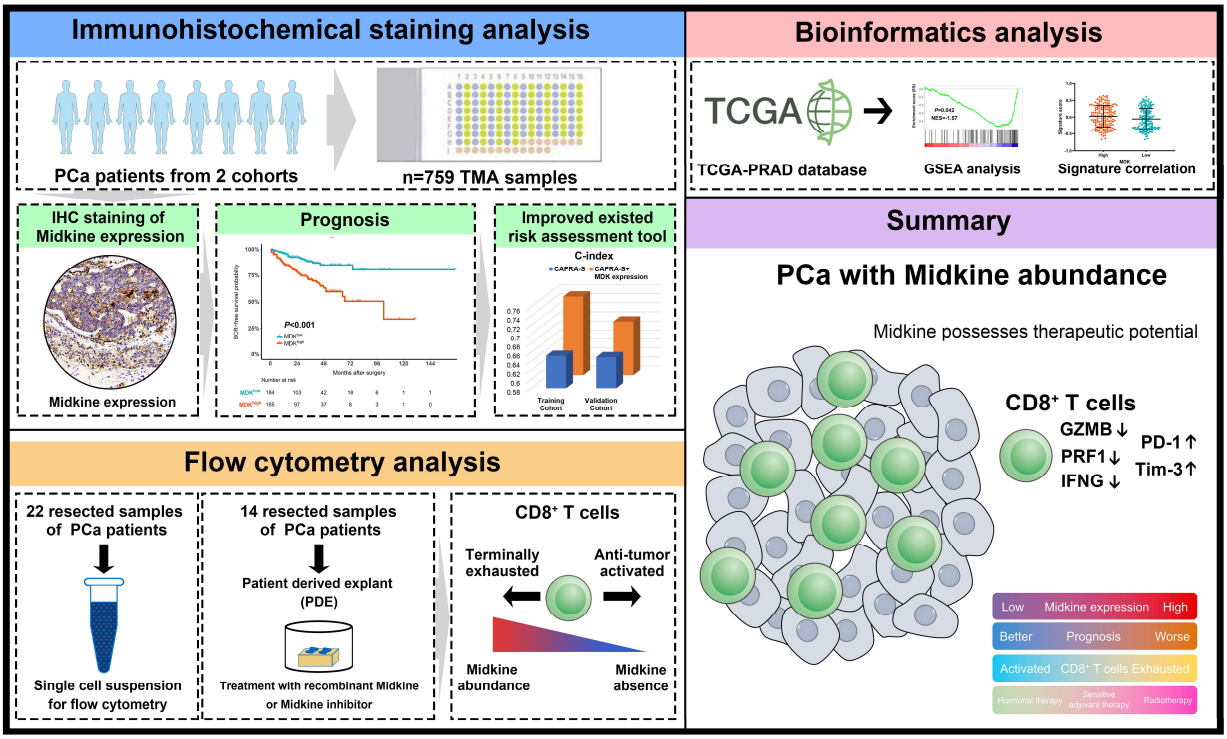

Supplementary Figure 10. Graphical abstract.

Supplementary Table 1. Flow cytometry antibodies.

No.	Marker	Dye	Antibody name	Clonality Species	Company	Product No.
1	CD45	APC-Cy7	APC-Cy7 Mouse Anti-Human CD45	Mouse Anti-human	BD Biosciences	557833
2	CD8	BB515	BB515 Mouse Anti-Human CD8	Mouse Anti-human	BD Biosciences	564526
3	CD3	BB515	BB515 Mouse Anti-Human CD56	Mouse Anti-human	BD Biosciences	552852
4	TNF	PE	PE Mouse Anti-Human TNF	Mouse Anti-human	BD Biosciences	559321
5	CD107A	AF647	AF647 Mouse Anti-Human CD107A	Mouse Anti-human	BD Biosciences	641581
6	IFN-γ	PE-Cy7	PE-Cy7 Mouse Anti-Human IFN-γ	Mouse Anti-human	BD Biosciences	557643
7	GZMB	AF647	AF647 Mouse anti-Human Granzyme B	Mouse Anti-human	BD Biosciences	560212
8	PRF-1	PE	PE Mouse Anti-Human Perforin	Mouse Anti-human	BD Biosciences	556437
9	Ki-67	BV421	BV421 Mouse Anti-Human Ki-67	Mouse Anti-human	BD Biosciences	562899
10	PD-1	PE-Cy7	PE-Cy7 Mouse Anti-Human PD-1	Mouse Anti-human	BD Biosciences	561272
11	Tim-3	PE	PE Mouse Anti-Human TIM-3 (CD366)	Mouse Anti-human	BD Biosciences	563422
12	PSMA	APC	APC Mouse Anti-Human PSMA Antibody	Mouse Anti-human	Biolegend	342508
13	LRP1	PE	PE Mouse Anti-Human CD91 (LRP1) Antibody	Mouse Anti-human	BD Biosciences	550497
14	LRP6	AF647	AF647 Mouse Anti-Human LRP6 Antibody	Mouse Anti-human	R&D Systems	FAB1505R

Supplementary Table 2. Gene signature applied in this study

Signature*	Source	Genes
Progenitor exhausted CD8$^+$ T cells signature	DOI: 10.1038/s41590-019-0312-6	*ARAP2, ASAP1, CD28, CD9, CRTAM, CXCL10, EEF1A1, EEF1B2, EEF1G, EHD3, EMB, EVL, FOSB, RPL35, GPR183, HIF1A, HSPE1, ICOS, ID3, IFIT3, IL7R, ITGB1, JUN, KCNN4, LIMD2, LTB, MIF, MS4A4A, MT-ATP6, MT-CO1, MT-CO2, MT-CO3, MT-CYB, MT-ND1, MT-ND2, MT-ND3, MT-ND4, MT-ND5, NACA, NEK7, NRP1, POU2F2, PTPN6, RILPL2, RNF213, RPL10A, RPL11, RPL13, RPL15, RPL22, RPL22L1, RPL23, RPL24, RPL26, RPL27A, RPL28, RPL29, RPL3, RPL30, RPL32, RPL34, RPL35, RPL35A, RPL36, RPL36A, RPL37, RPL4, RPL6, RPL7A, RPL8, RPLP0, RPLP1, RPLP2, RPS11, RPS14, RPS15, RPS15A, RPS16, RPS17, RPS18, RPS19, RPS2, RPS21, RPS27A, RPS28, RPS3A, RPS4X, RPS5, RPS6, RPS7, RPS8, RPS9, SLAMF6, SOCS3, TCF7, TNFSF8, TRAF1, USP18, WDR89, XCL2, ZFP36L1*
Terminally exhausted CD8$^+$ T cells signature	DOI: 10.1038/s41590-019-0312-6	*KIAA1671, ABI3, AKNA, APOBEC3H, ARHGAP9, ARL6IP1, ARMC7, BCL2A1, CBX4, CCL18, CCL4, CD160, CD164, CD27, CD3E, CD3G, CD7, CD82, CD8A, CST7, CXCR6, DAPK2, DTX1, DUSP2, EFHD2, EIF4A2, FAM189B, FASLG, FOXN3, FYN, GIMAP1, GIMAP6, GIMAP7, GLRX, GNG2, GRAMD1A, GZMA, GZMH, GZMK, HCST, HSPA5, ID2, IFIT3, IL21R, ISG15, ITK, ITPKB, LAG3, LAX1, LRRK1, MBNL1, MXD4, NR4A2, PDCD1, PFDN5, PLAC8, PRDX5, PRKCH, PSMB10, PSMB8, PSME1, PTGER4, PTPN18, PTPN22, RGS1, RGS2, RGS3, RTP4, RUNX3, SERPINA3, SERPINB6, SH2D2A, SHISA5, SIPA1, SLC3A2, STAT1, STK17B, TAPBP, TAPBPL, TNFRSF1B, TOX, UCP2, VMP1, ZBP1*
AR output score	DOI: 10.1016/j.cell.2015.10.025	*KLK3, TMPRSS2, NKX3-1, KLK2, GNMT, PMEPA1, MPHOSPH9, ZBTB10, EAF2, CENPN, C1orf116, ACSL3, PTGER4, ABCC4, NNMT, ADAM7, FKBP5, ELL2, MED28, HERC3*
AR activity signature	DOI: 10.1158/1078-0432.CCR-19-1587	*KLK3, KLK2, FKBP5, STEAP1, STEAP2, PPAP2A, RAB3B, ACSL3, NKX3-1*
Radiation Therapy Outcomes Score	DOI: 10.1016/S1470-2045(16)30491-0	*DRAM1, KRT14, PTPN22, ZMAT3, ARHGAP15, IL1B, ANLN, RPS27A, IRF4, TOP2A, GNG11, CDKN3, HCLS1, DTL, IL7R, UBA7, NEK1, CDKN2AIP, APEX2, KIF23, SULF2, PLK2, EME1, BIN2*

Supplementary Table 3. Univariate cox regression analyses of clinicopathological features associated with BCR-free survival.

	Training Cohort		Validation Cohort	
Characteristics	**HR (95% CI)**	***P***	**HR (95% CI)**	***P***
Age, per 1-y increase	0.999 (0.995-1.002)	0.502	0.999 (0.964-1.035)	0.945
Gleason score 7 vs. <7	2.709 (1.042-7.041)	**0.041**	2.372 (1.059-5.316)	**0.036**
Gleason score 8-10 vs. <7	4.778 (1.879-12.149)	**0.001**	4.672 (2.072-10.531)	**<0.001**
Preoperative PSA 10-20 vs <10	1.058 (0.573-1.955)	0.856	1.960 (1.015-3.785)	**0.045**
Preoperative PSA >20 vs <10	2.038 (1.166-3.560)	**0.012**	3.138 (1.675-5.881)	**<0.001**
Lymph node involvement	3.265 (1.659-6.427)	**0.001**	0.609 (0.085-4.380)	0.622
Positive surgical margin	1.498 (0.820-2.739)	0.189	0.403 (0.056-2.904)	0.367
Extracapsular extension	2.058 (0.983-4.305)	0.055	1.045 (0.565-1.931)	0.889
Seminal vesicle invasion	1.910 (1.128-3.235)	**0.016**	0.599 (0.147-2.438)	0.474
Peritumor MDK expression	1.276 (0.800-2.035)	0.306	1.185 (0.763-1.842)	0.450
Intratumor MDK expression	3.088 (1.837-5.194)	**<0.001**	2.789 (1.707-4.557)	**<0.001**

Abbreviations: CI, confidence interval; HR, hazard ratio; PSA, prostate specific antigen.

P value <0.05 marked in bold font shows statistical significance.

Supplementary Table 4. CAPRA-S score of training and validation cohorts

CAPRA-S score	Training Cohort (n=369)		Validation Cohort (n=390)	
	n	%	n	%
0	14	3.8	12	3.1
1	29	7.9	31	7.9
2	65	17.6	56	14.4
3	62	16.8	80	20.5
4	47	12.7	63	16.2
5	43	11.7	58	14.9
6	45	12.2	53	13.6
7	21	5.7	18	4.6
8	23	6.2	15	3.8
9	11	3.0	1	0.3
≥10	9	2.5	3	0.8